New type of high-frequency electrohydrodynamic instability in nematic liquid crystals

A. N. Trufanov, L. M. Blinov, and M. I. Barnik

Research Institute for Organic Intermediates and Dyestuffs
(Submitted 25 June 1979)
Zh. Eksp. Teor. Fiz. **78**, 622–631 (February 1980)

A new type of electrohydrodynamic instability in thin planarly oriented layers of nematic liquid crystal with negative dielectric anisotropy was experimentally observed and investigated. Its mechanism does not follow from the presently existing theoretical models. Characteristic features of this instability are a periodic director distribution perpendicular to the external field and stationary flow of the liquid in the plane of the liquid-crystal layer.

PACS numbers: 47.65. + a, 47.20. + m

1. INTRODUCTION

It is well known[1] that an electric field can produce in layers of nematic liquid crystals (NLC) various kinds of instability, which manifest themselves as spatially periodic pictures of the molecular orientation. The instability may be caused by flexoelectric[2,3] or electrohydrodynamic (EHD) destabilization of the NLC director. The known EHD instabilities can be divided into two types. The first includes those in which the destabilization is due to mechanisms that are typical also of isotropic liquids (these instabilities include the Felici injection instability[4] and the instability due to the electroconvective phenomena[5,6]). The second type includes the EHD instability due to a mechanism that is specific for an anisotropic medium (the Carr-Helfrich instability due to destabilization of the director on account of the moment induced by the anisotropy of the electric conductivity[7]).

Up to now, two regimes of Carr-Helfrich instability were investigated theoretically and experimentally.[8] At below-critical external-field frequencies ("conducting regime," $f<f_c$), a stationary picture of the director distribution is observed (the Kapustin–Williams domains) and a stationary rotational motion of the liquid. The volume charge oscillates in this case in time with the external field. At frequencies above critical ($f>f_c$), on the contrary, the space charge distribution is stationary and the motion of the director and of the liquid itself are in time with the field. This is the so-called "dielectric regime," which manifests itself in experiment in the form of a system of small domain lines (we shall call these "pre-chevron" domains; at voltages somewhat exceeding the threshold, a "chevron structure" is produced on them) and, as a rule, masked by the isotropic instability mode.[9] The frequency dependences of the threshold voltage (U_{thr}) of these instabilities, which are typical of NLC, have in the most general case the following form: for Kapustin–Williams domains there is a low-frequency plateau of $U_{\text{thr}}(f)$, which gives way to a sharp increase of U_{thr} as $f \to f_c$. For the "chevrons" one observes a square-root dependence of the threshold voltage on the frequency ($U_{\text{thr}} \sim f^{1/2}$).

There are also published reports[10,11] of observation, at high frequencies, of domain structures differing from those described above. However, they were not systematically studied, and the conditions or the mechanism for this instability were not made clear.

In this study we have experimentally investigated the behavior in a high-frequency electric field ($f>f_c$) of NLC with negative dielectric anisotropy, having relatively high electric conductivity (up to $10^{-7}\Omega^{-1}\text{cm}^{-1}$). It turns out that in this case it is possible to observe in planarly oriented layers a new EHD instability, due to the anisotropy of the electric conductivity of the NLC, but which does not follow from the earlier theoretical analysis.[8,12]

2. EXPERIMENTAL PROCEDURE

The experimental investigations of the instability were performed on flat sandwich-type cells, 4–200 μm thick. To obtain planar orientations, glasses with transparent SnO_2 electrodes were rubbed-on by the Chatelain method. We investigated three NLC with negative dielectric anisotropy ($\varepsilon_a = \varepsilon_\parallel - \varepsilon_\perp < 0$) and positive electric-conductivity anisotropy ($\sigma_a = \sigma_\parallel - \sigma_\perp > 0$): p-methoxybenzylindene-p'-butylaniline (MBBA) and p-butyl-p'-methoxyazoxybenzene (BMAOB), as well as the mixture[13] A (the subscripts $\parallel$ and $\perp$ pertain to the parallel and perpendicular directions relative to the director of the NLC). In addition, separate experiments were performed on p-butoxybenzylindene-p'-butylaniline (40.4) and p-butoxybenzylindene-p'-heptylaniline (40.7),[14], which have both nematic and smectic phases. Their dielectric anisotropy is also negative ($\varepsilon_a < 0$), and σ_a changes from positive to negative at a temperature (t^*) somewhat higher than the transition point (t_{NS}) into the smectic-A phase.

To change the dielectric anisotropy ε_a, small additions of p-cyanphenyl ester of p-heptylbenzoic acid (CEHBA) and 2,3-dicyan-4-amyloxyphenyl ester of p-amyloxybenzoic acid (DCEAA) were introduced into the initial NLC.[2] The electric conductivity σ and its anisotropy σ_a were varied by doping the NLC with tetrabutyl amonium bromide (TBAB), tetrabutyl amonium picrate (TBAP), and tetracyanethylene (TCE) in various concentrations.[13]

The threshold voltage E_{thr} of the onset of instability, and the period w of the domains, were determined visually with the aid of a polarization microscope, and

 0038-5646/80/020314-06$02.40

also by means of the diffraction pattern produced when a helium–neon laser beam ($\lambda = 632.8$ nm) passes through the cell. In addition, to determine E_{thr} we used a photoelectric method, in which we measured the dependence of the transmission of laser radiation through a cell with the NLC on the voltage on the cell. The accuracy of the determination of the E_{thr} and of the domain period w was ±5%. Whether the resultant instability is caused by static instability of the director or by EHD processes that accompany the flow of the liquid could be determined from the behavior of solid particles especially introduced into the NLC and of photochromic organic substances from the class of spiropyranes and dithizonates, dissolved in the NLC. In the latter case, the cell was illuminated directly in the course of observation under the microscope by a focused beam of a helium–cadmium laser ($\lambda = 441.6$ μm). These experiments were performed with a mixture, transparent in the 400–450 nm band, of phenylbenzoates[3] alloyed with DCEAA to obtain negative dielectric anisotropy. The character of the deformation of the director in the electric field is established from polarization investigations with the aid of a microscope. To this end, we investigated also the birefringence and its variation in a field, by probing the cell with a plane-parallel laser beam of 30 μm diameter. This made it possible to perform the measurements in a single domain.

3. RESULTS OF EXPERIMENT

The main condition for the appearance of new instability is a sufficiently high value of the electric conductivity in the NLC. The optically observed domain picture is shown in Fig. 1. The very first singularity of these domains is the large period, which exceeds the thickness of the NLC layer.

We introduce a coordinate frame xyz such that the xy plane coincides with the cell plane and the x axis with the initial direction of the director. In this case the directions of the light propagation (the observation direction) and of the applied external electric field coincide with the z axis. The domain fringes of this instability, just as the Kapustin–Williams domains and the "prechevron" domains are parallel to the y axis, i.e., perpendicular to the director. The domain picture has a maximum contrast in crossed polaroids, when the domains are seen in both parallel and perpendicular orientations of the director relative to the directions of the oscillations of the light passed by the polarizer.

In "white" light the domain picture comprises alternating light and dark fringes (Fig. 1a). The period of the domains at the threshold voltage is $w_{thr} \approx 1.5d$ (d is the thickness of the NLC layer). With increasing voltage, the width of the dark fringes decreases and that of the light ones increases. The system of parallel fringes is preserved up to voltages $U \approx 2U_{thr}$. When the cell is rotated about the z axis and viewed in crossed polaroids, the domain picture is gradually transformed. When the angle β between the NLC director and the plane of polarization of the light is $\gtrsim 5°$, the system of light and dark fringes has a period $w_{thr} \approx 3d$. At angles β close to 90°, the domains are again seen with a period $\sim 1.5d$. On the other hand, when a quartz compensating plate of first order is introduced (angle $\beta = 0$ or 90°), the domain picture acquires the form of a system of greenish-blue and orange-yellow fringes, that repeat with the same period $\sim 3d$. The form of the domain pattern for these two cases is shown in Fig. 1b. In the absence of an analyzer, no domain picture is observed. It becomes visible, however, when the cell is rotated around the x or y axis by an angle 10°, i.e., in the case of oblique incidence of the light on the cell, but only if the light is polarized along the x axis.

At voltages close to threshold and at normal incidence of the light on the cell, the diffraction pattern produced on the domain structure has two reflections, one on each side of the zeroth maximum. The diffraction angles and the intensities of the diffraction reflections remain practically unchanged when the cell is rotated around the z axis. For any cell position, the diffraction takes place in a plane containing the director. The polarization of the light in the ±2 reflection coincides with the polarization of the incident radiation, while in the ±1 reflection the polarizations are mutually perpendicular (the investigations were performed on MBBA with layer thickness 20 μm). It can therefore be concluded that each of these two reflections is of first order of diffraction by two different domain sublattices. The domain periods calculated from the condition for the maximum of the first order is $w_{thr} \approx 1.5d$ according to the ±2 reflection, and $w_{thr} \approx 3d$ according to the ±1 reflection. These data agree with the results of direct measurements with the microscope. In all the reflections there is weak modulation of the light at double the frequency of the applied electric field. The most appreciable modulation is observed for the ±1 reflection. The intensity of the light passing through the cell in crossed polaroids at angles β equal to 0 and 90° varies over the area of the cell when moving along the direction of the director, with a period $\sim 1.5d$. At angles β different from 0 and 90°, the periodicity of the transmission is $\sim 3d$. In these experiments the cell was probed with a narrow beam of light of 30 μm diameter (i.e., smaller than the width of a single domain).

Examination of the solid particles and of the cell sections colored by introducing photochromic matter shows that the appearance of the domain fringes is accompanied by motion of the liquid. The appearance of the visible domain picture practically coincides with the start of the motion. In two neighboring dark fringes (when observed with a quartz compensation plate, on the boundaries of the dark and light fringes) the liquid moves in mutually opposite directions in the xy plane

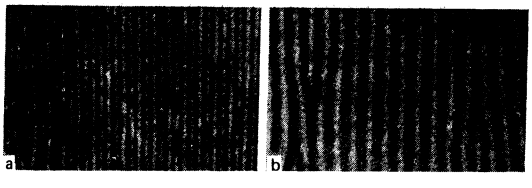

FIG. 1. Domain picture of the new type EHD instability (MBBA, doped with TCE; $\sigma_{\parallel} = 3 \cdot 10^{-8}\ \Omega^{-1}\text{cm}^{-1}$, $\sigma_{\parallel}/\sigma_{\perp} \approx 1.5$, $d = 12$ μm, $U = 60$ V, $f = 20$ kHz, $t = 22$ °C). Photograph dimensions 600 × 400 μm.

perpendicular to the initial director direction. These two fluxes are interconnected on the edges of the cell. No liquid motion is observed in other planes. A series of photographs showing the direction of motion of the liquid is given in Fig. 2. The photographs of the colored spot due to activation of the photochromic matter in the NLC and its variation under the influence of the flow were taken at different time intervals after application of the electric field to the cell. When the sample was heated, the motion of the liquid vanished directly at the point of transition of the NLC into the isotropic phase.

We note that in principle the shape of the spot colored by the photochromic admixture can vary with time also as a result of the anisotropy of the diffusion in the oriented NLC. This may suggest that the observed instability is the result of static deformation of the director, while the change in the shape of the spot is due to the anisotropy of the diffusion and is a reflection of only the character of the distribution of the director in the domain picture.

However, the picture of the spot deformation is such that it is impossible to visualize a corresponding deformation of the director. Furthermore, the anisotropy of the diffusion coefficients is small enough[15] (of the order of 1.6–1.7) and cannot explain such a strong spreading of the photochromic spot. Finally, so substantial diffusion of the admixture can take place within a time of the order of several seconds, since the average diffusion coefficient is only $\sim 10^{-7}$ cgs units.

Figure 3 shows the frequency characteristics of the threshold voltage for the onset of instability in MBBA at various electric conductivities and at a practically unchanged anisotropy of the electric conductivity. The curve 1 (lower electric conductivity) corresponds to the isotropic instability usually observed in NLC (pre-chevron domains)[5] wherein the threshold voltage has a frequency dependence $U_{thr} \sim f^{1/2}$. The low-frequency

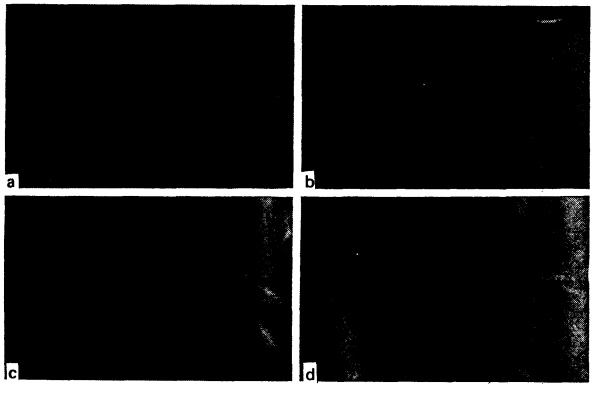

FIG. 2. Form of the domain picture of the EHD instability in a quartz compensation plate of first order and variation, in the field, of a colored spot due to activation of a photochromic impurity (mix of pheylbenzoates doped with DCEAA and TBAB; $\varepsilon_a = -0.5$, $\sigma_\parallel = 9 \cdot 10^{-10}$ Ω^{-1}cm^{-1}, $\sigma_\parallel/\sigma_\perp \approx 1.5$, $d = 65$ μm, $U = 200$ V, $f = 3$ kHz, $t = 22$ °C). Time after application of voltage, sec: *a*—0, *b*—5, *c*—10, *d*—20. Photograph dimensions 700 × 450 μm.

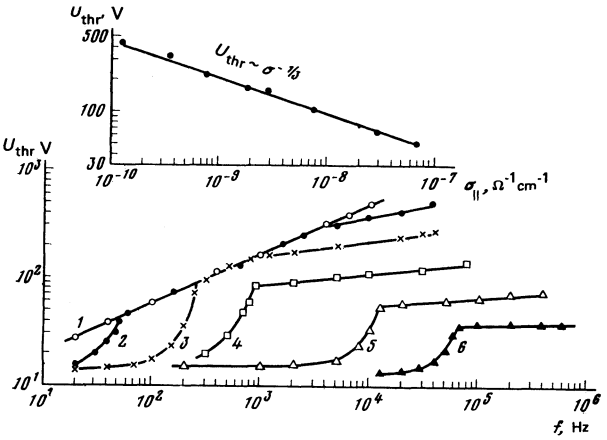

FIG. 3. Frequency characteristics of threshold voltage of EHD instability in MBBA at various electric conductivities ($t = 22$ °C, $\sigma_\parallel/\sigma_\perp \approx 1.15$, $d = 20$ μm). Conductivity, Ω^{-1}cm^{-1}: 1—$3 \cdot 10^{-11}$, 2—$2.7 \cdot 10^{-10}$, 3—$8 \cdot 10^{-10}$, 4—$2.9 \cdot 10^{-9}$, 5—$3 \cdot 10^{-8}$, 6—$2 \cdot 10^{-7}$. The inset shows the dependence of the threshold voltage on the electric conductivity ($f = 20$ kHz).

branches of all the remaining $U_{thr}(f)$ curves, with a characteristic sharp increase of the threshold voltage as $f \to f_c$, correspond to the threshold of formation of Kapustin–Williams domains. At intermediate electric conductivities (curves 2 and 3), at frequencies above critical (but not too high), pre-chevron domains are also observed with the characteristic square-root $U_{thr}(f)$ dependence. But at high frequencies (and for samples with high electric conductivity immediately beyond the critical frequency f_c, see curves 4–6), a new branch with a weak $U_{thr}(f)$ dependence appears. These threshold voltages correspond to the formation of the new domain instability described above.

In contrast to the pre-chevron instability and to the Kapustin–Williams domains, for which the threshold voltage does not depend on the electric conductivity, the threshold for the formation of the new type of domains decreases noticeably with increasing electric conductivity, like $U_{thr} \sim \sigma^{-1/3}$ (see the inset of Fig. 3). The threshold for the onset of the domains depends little on the thickness of the NLC layer and increases by approximately 1.5 times when the thickness is increased from 20 to 200 μm (Fig. 4). At voltages close to threshold, the domain period w_{thr} increases in proportion to the thickness of the NLC layer (see Fig. 4) and is practically independent of the frequency and magnitude (see Fig. 5) of the applied electric field. Far from the threshold ($U \gg U_{thr}$), however, the period of the domains, as seen from Fig. 5, decreases in proportion to U^{-2}. Thus, this is the second example (the first are the flux or electric domains[2,3,16]) of a domain-grating period controlled by an external field.

As already noted, the regime of instability with a threshold frequency characteristic $U_{thr} \sim f^{1/2}$ (curve 1 in Fig. 3) directly at the threshold corresponds to linear domains transverse to the director with a period of several microns.[5] Only when the voltage is increased is the domain picture deformed into a chevron structure.[1] If the branch of the threshold characteristic of

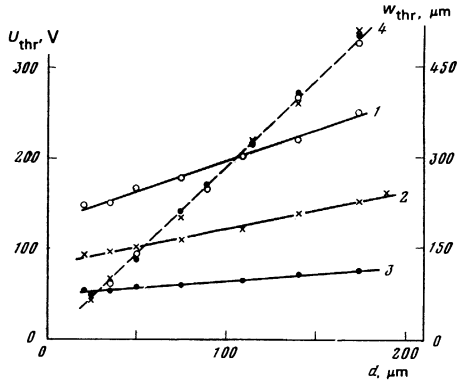

FIG. 4. Dependence of the threshold voltage (1–3) of the instability and of the period of the domains (4) on the thickness of the NLC layer (MBBA doped with TCE; $\sigma_{\parallel}/\sigma_{\perp} \approx 1.15$, $t = 23$ °C). Electric conductivity ($\Omega^{-1}\text{cm}^{-1}$) and frequency of the applied electric field (kHz) are respectively: 1—$8 \cdot 10^{-10}$,1; 2—$2.9 \cdot 10^{-9}$,2; 3—$3 \cdot 10^{-8}$,20; 4—$8 \cdot 10^{-10}$,2 (○); $2.9 \cdot 10^{-9}$, 2 (×); 3 $\cdot 10^{-8}$,20 (●).

the domains of the new type lies somewhat lower than the branch $U_{thr} \sim f^{1/2}$ (see, e.g., curve 4 of Fig. 3), then a chevron structure can also be produced, bypassing the linear-domain stage, against the background of the produced broad domain fringes, when the voltage is increased to values approximately coinciding with the $U_{thr} \sim f^{1/2}$ branch. The thin domain lines of the chevron instability in the dark fringes are then directed along the y axis, and bend gradually on going over into the region of the light fringes (see Fig. 6). At sufficiently high voltages at the center of the light fringes, they are directed practically along the x axis. If the electric conductivity of the NLC is so low that the threshold of the new-domains described here becomes higher than threshold of the pre-chevron linear domains, then the formation of the chevron structure from the latter takes place at voltages exceeding the threshold by 3–5 V, regardless of the further decrease of the electric conductivity. A chevron structure is produced near the critical frequency also by the Kapustin–Williams domains (the form of the domain picture reflecting this situation

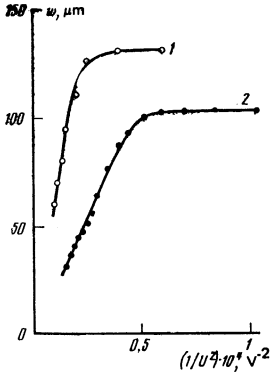

FIG. 5. Dependence of the period of the domains on the voltage across the NLC layer ($t = 23$ °C). 1—MBBA doped with TCE, $d = 45$ μm, $\sigma_{\parallel} = 2.9 \cdot 10^{-9}$ $\Omega^{-1}\text{cm}^{-1}$, $\sigma_{\parallel}/\sigma_{\perp} \approx 1.15$, $f = 20$ kHz; 2—MBBA, doped with TBAB, $d = 35$ μm, $\sigma_{\parallel} = 2.4 \cdot 10^{-9}$ $\Omega^{-1}\text{cm}^{-1}$, $\sigma_{\parallel}/\sigma_{\perp} \simeq 1.35$, $f = 4$ kHz.

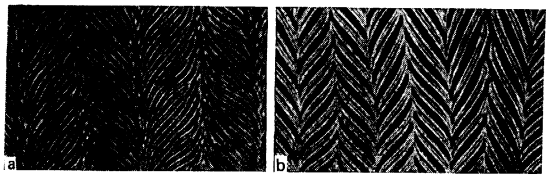

FIG. 6. "Chevron" structure produced from linear pre-chevron domains (*a*) and Kapustin–Williams domains (*b*): MBBA doped with TCE $\sigma_{\parallel} = 3 \cdot 10^{-11}$ (*a*) and 3×10^{-8} cm^{-1}, $U = 130$ (*a*) and 65 (*b*) V, $f = 40$ Hz (*a*) and 10 kHz (*b*), $\sigma_{\parallel}/\sigma_{\perp} \approx 1.15$, $d = 108$ μm, $t = 22$ °C. Dimensions of photographs 700×450 (*a*) at 450×300 (*b*) μm.

is shown in Fig. 6). This leads directly to a number of important conclusions. First, it is quite obvious that the formation of the chevron structure out of the linear pre-chevron domains and of the Kapustin–Williams domains is due to the onset of an instability of a new type. Second, these two types of instability (the domains of the new type, on the one hand, and the pre-chevron domains or Kapustin–Williams domains on the other) can exist simultaneously. Third, the formation of the pre-chevron domains stimulates the onset of the new type of instability.

The threshold voltage of the observed instability depends on the anisotropic parameters of the NLC. Experiment shows that with decreasing absolute value of ε_a (at $\varepsilon_a < 0$) the threshold voltage increases somewhat. Thus, a change of ε_a of MBAA from −2.8 to 0.02 by alloying it respectively with DCEAA and CEHBA leads to an increase of U_{thr} at 10 kHz from ~200 to ~240 V. We recall that the Kapustin–Williams have the opposite tendency.[17] The decrease of the anisotropy of the electric conductivity ($\sigma_{\parallel}/\sigma_{\perp} \to 1$) increases the instability threshold. This was demonstrated both by doping the NLC by various impurities, and by varying $\sigma_{\parallel}/\sigma_{\perp}$ by changing the temperature on a nematic phase with smectic short-range order [for the compounds (40.4) and (40.7)]. In the latter case the experimental data, as seen from Fig. 7, demonstrate convincingly that the $U_{thr}(\sigma_{\parallel}/\sigma_{\perp})$ curve diverges at the point $\sigma_{\parallel}/\sigma_{\perp} \to 1$. We note that in the temperature region where the anisotropy of the electric conductivity $\sigma_{\parallel}/\sigma_{\perp} < 1$, instability likewise sets in, with all the singularities typical of transverse (relative to the original orientation of the director) domains of the new type, which take place at $\sigma_{\parallel}/\sigma_{\perp} > 1$. At $\sigma_{\parallel}/\sigma_{\perp} < 1$, however, the domains are parallel to the director.

4. DISCUSSION OF RESULTS

Let us list the main features of the observed instability and the ensuing conclusions.

A. The instability has in practice a voltage threshold and a period proportional to the frequency of the NLC layer. From polarization investigations (the form of the domain picture in crossed polaroids with and without a quartz compensation plate, the formation of a chevron structure from the Kapustin–William domains and pre-chevron domains, etc.) it follows that the investigated instability is characterized by a periodic

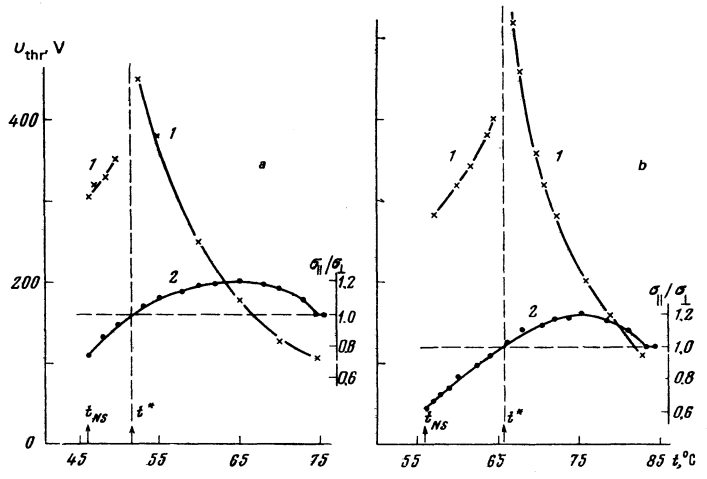

FIG. 7. Temperature dependences of the threshold voltage of domain instability (1) and anisotropy of the electric conductivity (2) for the samples (40.4) (*a*) and (40.7) (*b*) ($d = 35$ μm, $f = 10$ kHz (*a*) and 20 kHz (*b*).

distribution of the director in the *xy* plane. In addition, it appears that the director oscillates somewhat in the same plane about the equilibrium position at double the field frequency.

Assuming that the deformation of the director takes place also in the *xz* plane, we have attempted to observe it by means of the change of the phase delay in an electric field. At a light polarization vector orientation at an angle $\beta = 45°$ to the director, the experimental transmission curve should either oscillate or (if the molecule deviation is small) differ from the corresponding curve plotted for the angle $\beta = 0°$. No oscillations of the transmission curves were observed. The dependences of the light transmission on the voltage for one of the samples in crossed polaroids, at angles β equal to 0 and 45°, are shown in Fig. 8. The transmission curves for these angles are practically symmetrical. In the first case the transmission increases, and in the second it decreases, in full agreement with a deformation that takes place only in the *xy* plane. Thus, no symptoms of the expected deformation in the *xz* plane were observed. Consequently, there is either no deformation in the *xz* plane at all, or the deformation is too small and the sensitivity of the method too low to record it. The minimum deformation angle that could be observed in our experiment was 0.5–1°. We note

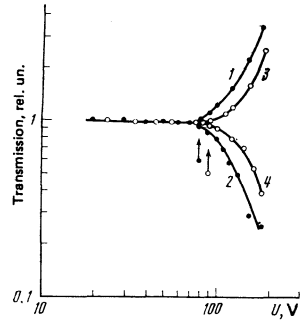

FIG. 8. Dependence of the light transmission on the voltage of a cell with MBBA doped with TCE in crossed polaroids ($\sigma_\parallel = 2.9 \cdot 10^{-9}\ \Omega^{-1}\text{cm}^{-1}$, $\sigma_\parallel/\sigma_\perp = 1.15$, $d = 35$ μm, $t = 25$ °C; 1 and 2—$\beta = 0$ and 45°, $f = 2$ kHz; 3 and 4—$\beta = 0$ and 45°, $f = 5$ kHz). The arrows show the threshold voltages for the onset of the domain picture.

also that the start of the deformation, determined by a photoelectric method in transmission, agrees within the limits of errors, with the threshold of the visually observed domain picture.

B. The instability is electrohydrodynamic, and the liquid of the motion has a stationary but quite unique character—the liquid flows in the *xy* plane perpendicular to the director (at $\sigma_a > 0$) and to the applied electric field. In the case of negative anisotropy of the electric conductivity ($\sigma_a < 0$), the liquid likewise flows in the *xy* plane, but along the director. Deformation of the molecular distribution in this case is observed only in the *xy* plane.

C. There is no instability in the isotropic phase. This fact, as well as the abrupt growth of the threshold voltage of the instability as $\sigma_a \to 0$ and the dependence of U_{thr} on ε_a indicate that this instability occurs only in anisotropic liquids. The decisive role in the mechanism of the onset of the instability is played by the anisotropy of the electric conductivity.

The presently existing theoretical models cannot describe this instability. However, the aggregate of the aforementioned symptoms suggests that the instability can be described by one of the versions of the Carr–Helfrich mechanism, when the EHD process is due to anisotropy of the electric conductivity. Solution of this problem calls for further investigation of the equations of the nematodynamics with allowance for the finite value of the electric conductivity, and possibly of the inertial term in the equation of motion of the liquid.[18]

The authors are grateful to S. A. Pikin and V. G. Chigrinov for helpful discussions of the possible instability mechanism, to N. I. Mashirina for the dielectric measurements of the investigated NLC samples, as well as to N. I. Bolondaeva for supplying the samples of the photochromic materials.

[1]L. M. Blinov, Élektro- i magnitooptika zhidkikh kristallov (Electro- and Magnetooptics of Liquid Crystals), Nauka, 1978.

[2]M. E. Barnik, L. M. Blinov, A. N. Trufanov, and B. A. Umanskiĭ, Zh. Eksp. Teor. Fiz. 73, 1936 (1977) [Sov. Phys.

JETP **46**, 1016 (1977)].
[3]M. I. Barnik, L. M. Blinov, A. N. Trufanov, and B. A. Umanski, J. Phys. (Paris) **39**, 417 (1978).
[4]N. Felici, Rev. Gen. Elect. **78**, 17 (1969).
[5]M. I. Barnik, L. M. Blinov, M. F. Crebenkin, and A. N. Trufanov, Mol. Cryst. Liq. Cryst. **37**, 47 (1976).
[6]M. I. Barnik, L. M. Blinov, S. A. Pikin, and A. N. Trufanov, Zh. Eksp. Teor. Fiz. **72**, 756 (1977) [Sov. Phys. JETP **45**, 396 (1977)].
[7]W. Helfrich, J. Chem. Phys. **51**, 4092 (1969).
[8]E. Dubois-Violette, P. G. de Gennes, and O. Parodi, J. Phys. (Paris) **32**, 305 (1971).
[9]R. Ribotta and G. Durand, J. Phys. (Paris) **40**, Collog. C3-334 (1979).
[10]A. A. Bronnikova and E. A. Kirsanov, 2nd All-Union Sci. Conf. on Liquid Crystals, Ivanovo, 1973, p. 133.
[11]P. Petrescu and M. Giurgea, Phys. Lett. **59A**, 41 (1976).
[12]I. W. Smith, Y. Galerne, S. T. Lagerwall, E. Dubois-Violette, and G. Durand, J. Phys., Collog. **36**, C1-237 (1975).
[13]M. I. Barnik, S. V. Belyaev, M. F. Grebenkin, V. G. Rumyantsev, V. A. Seliverstov, V. A. Tsvetkov, and N. M. Shytkov, Kristallografiya **23**, 805 (1978) [Sov. Crystallogr. **23**, 451 (1978)].
[14]L. M. Blinov, M. I. Barnik, V. T. Lazareva, and A. N. Trufanov, J. Phys. (Paris) **40**, Collog. C3-263 (1979).
[15]F. Rondelez, Solid State Commun. **14**, 815 (1974).
[16]L. K. Vistin', Dokl. Akad. Nauk SSSR **194**, 1318 (1974) [Sov. Phys. Dokl. **15**, 908 (1975)].
[17]M. I. Barnik, L. M. Blinov, M. F. Grebenkin, S. A. Pikin, and V. G. Chigrinov, Zh. Eksp. Teor. Fiz. **69**, 1080 (1975) [Sov. Phys. JETP **42**, 554 (1975)].
[18]S. A. Pikin and V. G. Chigrinov, Zh. Eksp. Teor. Fiz. **78**, 246 (1980) [Sov. Phys. JETP **51**, 123 (1980)].

Translated by J. G. Adashko

Nature of localized magnetic moments in band antiferromagnets

B. S. Volkov and M. S. Nunaparov

P. N. Lebedev Physics Institute, USSR Academy of Sciences
(Submitted 14 July 1979)
Zh. Eksp. Teor. Fiz. **78**, 632–639 (February 1980)

It is shown that a nonmagnetic interaction of an impuity atom with a spin-density wave of band electrons of an antiferromagnet leads to formation of an electron state, localized on the impurity, with an uncompensated spin. The phenomenon takes place because the interaction with the impurity violates the equivalence of the electronic spin subbands and is analogous in many respects of excitonic ferromagnetism. The localized magnetic field is calculated as a function of the position of the Fermi level. The results of the model can be easily applied to the case of exchange interaction between a magnetic impurity and a charge-density wave, and can describe the screening of the bare magnetic moment of the impurity by the spins of the band electrons (in analogy with the Kondo effect). The proposed theory explains the nature of the magnetic moments of certain impurities of other lattice defects. The theory is compared with experimental data obtained for chromium alloys.

PACS numbers: 75.10.Jm, 75.50.Ee

1. We propose in this paper a model for the production of a localized magnetic moment in systems with electron–hole pairing.[1,2] In these systems, as a result of the special properties of the electron spectrum (the presence of congruent sections of the Fermi surfaces of the electrons and holes), even an arbitrarily weak electron–hole interaction leads, with decrease of temperature, to substantial changes in the electron subsystem. Below a certain temperature T_c a long-range order is produced in the system and is characterized by a parameter Δ. The value of Δ is proportional to the density of the condensate of the electron–hole pairs.

Depending on the nature of the electron–hole interaction, different types of spin structure of the ordered state are possible.[2] In the case of singlet pairing, the order parameter Δ_s is independent of the spin and corresponds to formation of a charge density wave (CDW) in the system. Pairing of electrons in the triplet state leads to formation of a spin-density wave (SDW). In this case the spin structure of the order parameter takes the form $\Delta_t=(\Delta\cdot\sigma_{\alpha\beta})$, where $\sigma_{\alpha\beta}$ are 2×2 Pauli matrices. It is known[3,4] that the formation of the SDW is reflected in the antiferromagnetic behavior of chromium.

Introduction of an impurity atom in a system with SDW leads to a local redistribution of the spin of the band electrons such that in the vicinity of the impurity there appears a nonzero magnetic moment. When analysing the influence of the impurity on the electron subsystem of the metal, a distinction must be made between two types of interaction of the electrons with the impurity atom.

If the impurity does not have a magnetic moment, then its interaction with the band electrons is described by the usual potential scattering $V(\mathbf{r})\Psi_\alpha+\Psi_\alpha(\Psi_\alpha^+$ is the operator of production of a particle with spin α).

 0038-5646/80/020319-05$02.40